This article was downloaded by:
On: *25 January 2011*
Access details: *Access Details: Free Access*
Publisher *Taylor & Francis*
Informa Ltd Registered in England and Wales Registered Number: 1072954 Registered office: Mortimer House, 37-41 Mortimer Street, London W1T 3JH, UK

Separation Science and Technology
Publication details, including instructions for authors and subscription information:
http://www.informaworld.com/smpp/title~content=t713708471

Orthogonal Curvilinear Cake Filtration

George G. Chase[a]; Max S. Willis[a]
[a] DEPARTMENT OF CHEMICAL ENGINEERING, THE UNIVERSITY OF AKRON, AKRON, OHIO

To cite this Article Chase, George G. and Willis, Max S.(1991) 'Orthogonal Curvilinear Cake Filtration', Separation Science and Technology, 26: 5, 689 — 715
To link to this Article: DOI: 10.1080/01496399108049909
URL: http://dx.doi.org/10.1080/01496399108049909

PLEASE SCROLL DOWN FOR ARTICLE

Full terms and conditions of use: http://www.informaworld.com/terms-and-conditions-of-access.pdf

This article may be used for research, teaching and private study purposes. Any substantial or systematic reproduction, re-distribution, re-selling, loan or sub-licensing, systematic supply or distribution in any form to anyone is expressly forbidden.

The publisher does not give any warranty express or implied or make any representation that the contents will be complete or accurate or up to date. The accuracy of any instructions, formulae and drug doses should be independently verified with primary sources. The publisher shall not be liable for any loss, actions, claims, proceedings, demand or costs or damages whatsoever or howsoever caused arising directly or indirectly in connection with or arising out of the use of this material.

SEPARATION SCIENCE AND TECHNOLOGY, 26(5), pp. 689–715, 1991

Orthogonal Curvilinear Cake Filtration

GEORGE G. CHASE* and MAX S. WILLIS
DEPARTMENT OF CHEMICAL ENGINEERING
THE UNIVERSITY OF AKRON
AKRON, OHIO 44325-3906

Downloaded At: 12:42 25 January 2011

Abstract

Conventional analysis of cake filtration considers cakes formed under one-dimensional rectilinear flow conditions. Other cake geometries are often encountered in practice, and more generalized equations are needed. An orthogonal curvilinear filter cake equation is derived here for an arbitrary orthogonal cake geometry. This equation is applied to rectangular, cylindrical, oblate-spheroidal, and elliptic-cylindrical geometry cakes through the coordinate scale factors. Experiments are run on Lucite cakes in rectangular and elliptic-cylindrical coordinates. The constitutive parameter, λ, is determined from experiments in rectangular coordinates and is used to predict the performance of an elliptic-cylindrical cake. Comparison of the predicted results with the experimental results of the elliptic-cylindrical cake shows the consistency of the equation for different geometries. The filter assembly used in the experiments was designed to be pressurized without being submerged within a larger slurry agitation vessel. This allows ready access to the assembly walls for placement of probes for measuring local pressure and porosity in rectangular and elliptic-cylindrical geometries.

INTRODUCTION

Conventional analysis of filter cakes considers only one-dimensional flow conditions in which the growing cake surface remains parallel to the flat filter medium. Other cake geometries are often encountered in practice, and a more generalized filter equation is needed for other geometries.

Yoshioka et al. (*21*) point out that all pressure-driven cake filtrations are actually one-dimensional flow filtrations. The velocity streamlines follow one coordinate while the other two coordinates lie in the uniform pressure surfaces normal to the velocity streamlines. Brenner (*2*) shows that unconfined cakes formed on circular leaf membranes are best described in oblate-spheroidal coordinates. Others have extended his work

*To whom correspondence should be addressed.

Copyright © 1991 by Marcel Dekker, Inc.

to include cakes forming in spherical, cylindrical, and elliptic-cylindrical geometries. A partial list of orthogonal curvilinear filter cakes reported in the literature is given in Table 1.

In the literature the theoretical governing equations are derived separately for each particular geometry as an *ad hoc* extension of the conventional analysis. Shirato et al. (*15*) recognize the similarity between the derived equations for the different geometries and define an effective filtration area (EFA) factor to make the equations analogous. While the EFA is useful, it is based on the *ad hoc* models and their inherent limitations.

The volume-averaged continuum theory provides a more rigorous approach to obtain the governing equations for cake filtration. This approach has been used to obtain the governing equation for one-dimensional cake filtration (*20*) and is used here for orthogonal curvilinear filter cakes. In the application of the continuum equations, restrictive assumptions become explicit. Furthermore, the analysis can be readily extended to include other effects, such as mass transfer between the phases or heterogeneous chemical reactions, by including terms that the assumptions have removed.

The results of the experiments are expressed in terms of the volume-averaged parameters used in the orthogonal curvilinear cake governing equation. Expressing the results in terms of the *ad hoc* EFA is not necessary in showing the usefulness of the volume-averaged approach.

Downloaded At: 12:42 25 January 2011

TABLE 1
Orthogonal Curvilinear Cake Geometries Reported in the Literature

Authors	Curvilinear coordinates
Brenner (*2*)	Oblate-spheroidal
Leonard and Brenner (*11*)	Oblate-spheroidal
Shirato et al. (*15*)	Cylindrical
	Elliptic-cylindrical
	Oblate-spheroidal
	Spherical
Shirato and Kobayashi (*14*)	Cylindrical
	Elliptic-cylindrical
	Oblate-spheroidal
	Spherical
Yoshioka et al. (*21*)	Cylindrical
	Spherical
Gregor and Scarlett (*7*)	Oblate-spheroidal
Murase et al. (*12*)	Cylindrical
Tiller and Yeh (*17*)	Cylindrical
Bybyk (*3*)	Oblate-spheroidal

Experimentally, local pressure and porosity measurements are difficult to obtain in orthogonal curvilinear cakes due to the geometric shapes. As a result, few of the data reported in the literature include local measurements. Yoshioka et al. (*21*), Murase et al. (*12*), and Bybyk (*3*) measure local pressure in several geometries by inserting small pressure probe tubes into the cake. None of the reported data include local porosity measurements.

The experimental work here shows that it is possible to make local pressure and porosity measurements with pressure taps and porosity probes flush in the walls of the filter assembly of an elliptic-cylindrical filter cake. The experimental results show consistency between the rectangular and elliptic-cylindrical cake geometries as required by the governing equation for orthogonal curvilinear coordinates.

TERMINOLOGY

Conventional descriptions of filter cakes are based on the cake growth directions. A cake in which the cake-slurry surface is parallel to a flat filter medium and grows in a direction normal to the medium is referred to as a one-dimensional or a unidimensional filter cake. Similarly, a cake that grows in all three rectangular directions is referred to as a three-dimensional or a nonunidimensional filter cake (*2*, *7*, *11*, *12*, *14*, *15*).

A different terminology is introduced here based on the description of the flow streamlines instead of the cake growth directions. A conventional unidirectional cake with straight and parallel streamlines is referred to here as a rectilinear cake. A conventional nonunidirectional cake with curved and nonparallel streamlines is referred to here as an orthogonal curvilinear cake.

In some cakes the effects of nonisotropic properties may cause the streamlines and pressure surfaces to be nonorthogonal. However, conclusive experimental evidence of such nonorthogonality is not available. For the purposes of this work, such effects are assumed to be minor and the new rectilinear and orthogonal curvilinear terminology are sufficient for the cakes being considered here.

THE ORTHOGONAL CURVILINEAR FILTER CAKE EQUATION

The volume-averaging approach to modeling flows through porous media is well known (*1*, *5*, *8–10*, *16*). The important effects in isothermal cake filtration are accounted for in the mass and momentum balances for the solid and fluid phases. These balances are evaluated to obtain the orthogonal curvilinear filter cake equation. Rectilinear flow filter cakes are a special case of this generalized equation.

Table 2 lists the mass and momentum balances and constitutive relations

Downloaded At: 12:42 25 January 2011

TABLE 2
Volume Averaged Continuum Scale Mass and Momentum Balances and Constitutive Relations

Continuum balances	
Mass:	
$$\frac{\partial}{\partial t}\epsilon_\alpha + \nabla\cdot(\epsilon_\alpha \mathbf{v}^\alpha) = 0, \qquad \alpha = f, s$$	(1)
Momentum:	
$$\frac{\partial}{\partial t}(\epsilon_\alpha \rho^\alpha \mathbf{v}^\alpha) + \nabla\cdot(\epsilon_\alpha \rho^\alpha \mathbf{v}^\alpha \mathbf{v}^\alpha) + \nabla\cdot\mathbf{t}^\alpha + \epsilon_\alpha \rho^\alpha \hat{\mathbf{T}}^\alpha - \epsilon_\alpha \rho^\alpha \mathbf{g} = 0$$	(2)
where $$\mathbf{t}^\alpha = \langle \mathbf{t} \rangle_\alpha + \frac{1}{dV}\int_{dV} \rho_\alpha \tilde{\mathbf{v}}^\alpha \tilde{\mathbf{v}}^\alpha \, dv$$	(3)
$$\hat{\mathbf{T}}^\alpha = \frac{1}{\langle \rho_\alpha \rangle dV}\int_{dA_{fs}} \mathbf{t}\cdot\mathbf{n}^{fs} \, da$$	(4)
Constitutive relations	
$$\mathbf{t}^\alpha = \epsilon_\alpha p^f \boldsymbol{\delta} + \boldsymbol{\tau}^\alpha$$	(5)
$$\epsilon_\alpha \rho^\alpha \hat{\mathbf{T}}^\alpha = -p^f \nabla(\epsilon_\alpha) + \hat{\boldsymbol{\tau}}^\alpha$$	(6)
$$\hat{\boldsymbol{\tau}}^f = -\hat{\boldsymbol{\tau}}^s = -\boldsymbol{\lambda}(\mathbf{v}^f - \mathbf{v}^s), \qquad \boldsymbol{\lambda} = \boldsymbol{\lambda}(\rho^f, \epsilon_f)$$	(7)

from the theory (*10*). The superscript and subscript α in these equations represents either the fluid (f) or the solid (s) phases. In this table, ϵ_α is the local porosity or volume fraction occupied by the α-phase; ρ^α is the α-phase intrinsic mass density; $\mathbf{v}^\alpha$ is the intrinsic α-phase mass averaged velocity vector; $\mathbf{t}^\alpha$ is the average stress tensor; $\hat{\mathbf{T}}^\alpha$ is the momentum transfer vector function between the phases; $\boldsymbol{\tau}^\alpha$ and $\hat{\boldsymbol{\tau}}^\alpha$ are the dissipative stress and drag force parts of $\mathbf{t}^\alpha$ and $\hat{\mathbf{T}}^\alpha$; p^f is the fluid-phase pressure; $\mathbf{g}$ is the acceleration due to gravity; and $\boldsymbol{\lambda}$ is the material coefficient tensor or resistance tensor.

Within the interstices between the particles, the phase velocities and their deviations cannot be measured. As a result, the observable averaged stress tensor is the sum of the averaged microscale stress tensor and the deviation convective term as given in Eq. (3). This is consistent with the work by Hassanizadeh and Gray (*10*).

Dimensional analysis (*18*) and experimental measurements (*6*) show that

Downloaded At: 12:42 25 January 2011

the dominant forces in the fluid-phase momentum balance are the pressure and drag forces. In large cakes or large material densities, gravity can also become important. For the purposes here, it is assumed insignificant.

Combining Eq. (2) with the constitutive relations, Eqs. (5) and (6), and neglecting the insignificant terms gives

$$\epsilon_f \nabla(p^f) + \hat{\tau}^f = 0 \tag{8}$$

as the fluid-phase momentum balance which is implicitly a function of time.

Orthogonal Curvilinear Coordinates

The governing equation for an orthogonal curvilinear filter cake is obtained by assuming the cake geometry is described by the orthogonal curvilinear coordinate system (q_1,q_2,q_3) where the velocity streamlines coincide with the q_1 coordinate direction. This is shown in Fig. 1. As Yoshioka et al. (*21*) point out, this means that the pressure and porosity are only functions of the q_1 coordinate.

The conversion of the mass and momentum balances, Eqs. (1) and (8), into the orthogonal curvilinear coordinate system requires the use of the scale factors, h_i, defined by (*13*)

$$h_i^2 = \sum_j (\partial x_j/\partial q_i)^2 \tag{9}$$

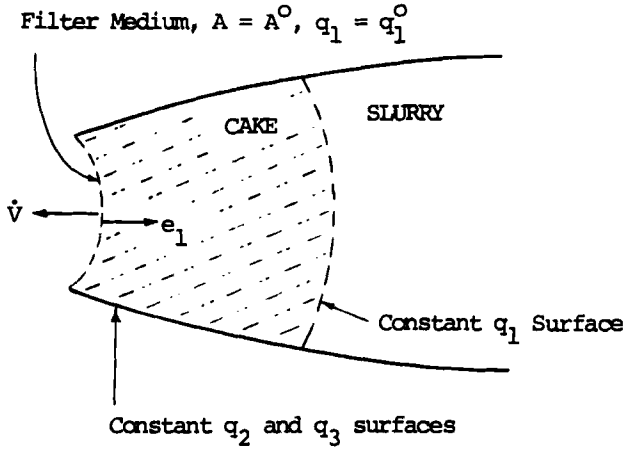

FIG. 1. Orthogonal curvilinear geometry filter cake with flow in the $-q_1$ direction.

Downloaded At: 12:42 25 January 2011

where x_j ($j = 1, 2, 3$) are the rectangular coordinates (x,y,z). The expressions

$$(\nabla f)_i = \frac{1}{h_i}\frac{\partial f}{\partial q_i} \qquad (i \text{ not summed}) \tag{10}$$

$$\nabla\cdot\mathbf{f} = \frac{1}{h_1h_2h_3}\left[\frac{\partial(f_1h_2h_3)}{\partial q_1} + \frac{\partial(f_2h_1h_3)}{\partial q_2} + \frac{\partial(f_3h_1h_2)}{\partial q_3}\right] \tag{11}$$

are the transformations for gradients and divergences, respectively.

The mass balance, Eq. (1), in q_i coordinates becomes

$$\frac{\partial\epsilon_\alpha}{\partial t} + \frac{1}{h_1h_2h_3}\frac{\partial}{\partial q_1}(h_2h_3\epsilon_\alpha v_1^\alpha) = 0, \qquad \alpha = f, s \tag{12}$$

where the velocity components in the q_2 and q_3 directions are zero due to the assumption that the velocity streamlines coincide with the q_1 coordinate. Similarly, the momentum balance, Eq. (8), is

$$\frac{\epsilon_f}{h_1}\frac{\partial p^f}{\partial q_1} + \hat{\tau}_1^f = 0 \tag{13}$$

where, due to the lack of experimental evidence to the contrary in cake filtration, the q_2 and q_3 components of the drag force, $\hat{\tau}^f$, are assumed to be insignificant. The constitutive relation, Eq. (5), reduces to

$$\hat{\tau}_1^f = -\lambda(v_1^f - v_1^s) \tag{14}$$

where λ_{11} is written as λ to simplify the notation.

The Generalized Orthogonal Curvilinear Filter Cake Equation

Combining Eqs. (13) and (14) gives the fluid-phase momentum balance as

$$\frac{\epsilon_f}{h_1}\frac{\partial p^f}{\partial q_1} - \lambda(v_1^f - v_1^s) = 0 \tag{15}$$

which is implicit in time and explicit in velocity.

Willis and Tosun (*20*) and Willis et al. (*18*) show that for a rectilinear cake the governing filter cake equation can be obtained by evaluating the

Downloaded At: 12:42 25 January 2011

momentum balance at the medium. The same approach is applied to an oblate-spheroidal cake by Bybyk (*3*) and is applied here to an arbitrary orthogonal curvilinear filter cake.

Before evaluating Eq. (15) at the cake–medium boundary, it is first transformed into a dimensionless coordinate and integrated over the cross-sectional area normal to the q_1 direction. The dimensionless coordinate, ξ, is defined as the fractional cake volume

$$\xi \equiv V_p/V_c \tag{16}$$

where the partial volume of the cake in Fig. 1 is given by

$$V_p = \int_{q_1^0}^{q_1} \int_{q_2^0}^{q_2^c} \int_{q_3^0}^{q_3^c} h_1 h_2 h_3 \, dq_1 dq_2 dq_3 \tag{17}$$

and where V_p is only a function of q_1. The volume of the whole cake, V_c, is obtained by evaluating V_p at q_1^c. By applying the chain rule for differential calculus, the derivative of the pressure becomes

$$\frac{\partial P}{\partial q_1} = \frac{1}{V_c} \frac{dV_p}{dq_1} \frac{\partial P}{\partial \xi} \tag{18}$$

where p^f in Eq. (15) is replaced by P to simplify the notation.

Substituting Eq. (18) into Eq. (15), integrating over the area, and evaluating at the medium gives

$$\left[\int_{q_2^0}^{q_2^c} \int_{q_3^0}^{q_3^c} \frac{\epsilon_f}{h_1} \frac{1}{V_c} \frac{dV_p}{dq_1} \frac{\partial P}{\partial \xi} \, dq_2 dq_3 \right]_{q_1^0} - \left[\int_{q_2^0}^{q_2^c} \int_{q_3^0}^{q_3^c} h_2 h_3 \lambda (v_1^f - v_1^s) \, dq_2 dq_3 \right]_{q_1^0} = 0 \tag{19}$$

Since the porosity, velocities, pressure, and the material coefficient are only functions of q_1, then Eq. (19) simplifies to

$$\frac{\epsilon_f^0}{V_c} \left[\frac{dV_p}{dq_1} \right]^0 \left[\frac{\partial P}{\partial \xi} \right]^0 \int_{q_2^0}^{q_2^c} \int_{q_3^0}^{q_3^c} \left[\frac{h_2 h_3}{h_1} \right]^0 dq_2 dq_3 - \lambda^0 (v_1^f - v_1^s)^0 A^0 = 0 \tag{20}$$

where a superscript "0" implies that the term is evaluated at the cake–medium boundary. The area, A^0, is the surface area at the medium. The

Downloaded At: 12:42 25 January 2011

area at any position q_1 is given by

$$A(q_1) = \int_{q_2^0}^{q_2^f} \int_{q_3^0}^{q_3^f} (h_2 h_3)_{q_1} \, dq_2 dq_3 \tag{21}$$

where the notation $(h_2h_3)_{q_1}$ indicates that the product (h_2h_3) is evaluated at the q_1 position.

The solid-phase particles are stopped by the filter medium and hence the solid-phase velocity at the medium is zero. A fluid-phase mass jump balance at the medium gives the boundary condition

$$v_1^{f0} A^0 = -\dot{V}/\epsilon_f^0 \tag{22}$$

where $\dot{V}$ is the filtrate volumetric flow rate. The minus sign accounts for the velocity in the minus q_1 direction while $\dot{V}$ is defined as a positive quantity.

To obtain the general curvilinear filter cake equation, a dimensionless pressure gradient at the medium is defined as

$$J_0 \equiv \frac{1}{P_c} \left[\frac{\partial P}{\partial \xi} \right]^0 \tag{23}$$

where P_c is the pressure drop across the whole cake. Also, a geometric shape factor, h, is defined by

$$h \equiv \frac{(A^0)^2}{\left[\dfrac{dV_p}{dq_1}\right]^0 \displaystyle\int_{q_2^0}^{q_2^f} \int_{q_3^0}^{q_3^f} \left[\frac{h_2 h_3}{h_1}\right]^0 dq_2 dq_3} \tag{24}$$

which is a constant depending on the cake coordinate geometry.

Combining Eqs. (22)–(24) with Eq. (20) gives the orthogonal curvilinear filter cake equation

$$P_c = -\left[\frac{h\lambda^0}{(\epsilon_f^0)^2 J_0}\right] \frac{V_c \dot{V}}{(A^0)^2} \tag{25}$$

which relates the cake pressure drop to the filtrate rate and cake volume.

Ratio of Cake and Filtrate Volumes

The conventional analysis of cake filtration normally relates the pressure drop and the filtrate rate to the filtrate volume instead of the cake volume

Downloaded At: 12:42 25 January 2011

as is given in Eq. (25). An expression for relating these two volumes is obtained from the mass balance.

The cake–filtrate volume ratio, G, is defined as the ratio of the time rates of change of the filtrate and cake volumes:

$$G \equiv \dot{V}_c/\dot{V} \tag{26}$$

Since both the cake and the filtrate volumes are only functions of time, then Eq. (26) may be written as

$$G = dV_c/dV \tag{27}$$

where V_c and V are the instantaneous cake and filtrate volumes. When G is constant and the initial filtrate volume is zero, Eq. (27) can be integrated to obtain

$$G = V_c/V \tag{28}$$

The volume ratio, G, is related to the slurry porosity, ϵ_f^s, and cake average porosity, ϵ_f^*, by the expression

$$G = (1 - \epsilon_f^s)/(\epsilon_f^s - \epsilon_f^*) \tag{29}$$

which is obtained by integrating the fluid-phase mass balance over the whole cake (*4*, *20*). This expression assumes that the time rate of change of the cake average porosity is negligible (*19*) and that the velocities of the two phases are equal in the slurry above the cake.

Substitution of Eq. (28) into Eq. (25) gives

$$P_c = -\left[\frac{h\lambda^0}{(\epsilon_f^0)^2 J_0}\right]\frac{GV\dot{V}}{(A^0)^2} \tag{30}$$

which relates the cake pressure drop and the filtrate rate to the filtrate volume as in the conventional analysis. The difference here is that Eq. (30) is applicable to any orthogonal curvilinear flow filter cake.

Equations for Specific Geometries

Four cake geometries are shown in Fig. 2 for a rectilinear flow cake in rectangular coordinates and curvilinear flow cakes in cylindrical, oblate-spheroidal, and elliptic-cylindrical coordinates. The corresponding scale factors and values or expressions for terms in the orthogonal curvilinear filter cake equation, Eq. (25), are listed in Table 3.

Downloaded At: 12:42 25 January 2011

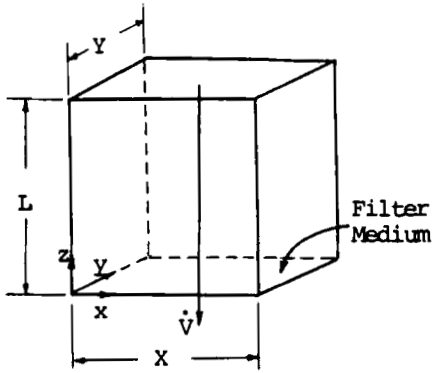

(a) Rectangular Cake. Rectilinear flow in (-z) direction.

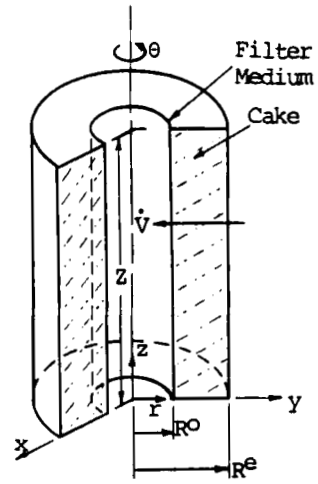

(b) Cylindrical Cake. Curvilinear flow in (-r) direction.

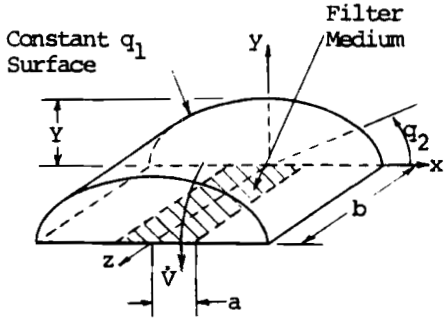

(c) Oblate-Spheroidal Cake. Curvilinear flow in ($-q_1$) direction.

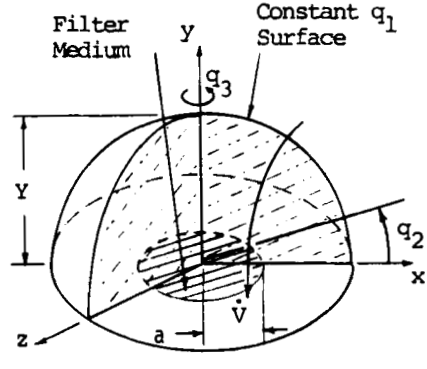

(d) Elliptic-Cylindrical Cake. Curvilinear flow in ($-q_1$) direction.

FIG. 2. Rectangular, cylindrical, oblate-spheroidal, and elliptic-cylindrical filter cake geometries.

Downloaded At: 12:42 25 January 2011

TABLE 3
Coordinate Relations, Scale Factors, and Expressions for the Cake Geometries in Figure 2

Rectangular cake: Rectilinear flow in $(-z)$ direction	
Coordinate relations and limits	$x = x, \quad 0 \le x \le X$ $y = y, \quad 0 \le y \le Y$ $z = z, \quad 0 \le z \le L$
Scale factors	$h_x = h_y = h_z = 1$
Medium area	$A^0 = XY$
Cake volume	$V_c = XYL$
Shape factor	$h = 1$
Dimensionless pressure gradient	$J_0 = \frac{L}{P_c}\left(\frac{\partial P}{\partial z}\right)_{z=0}$
Oblate-spheroidal cake: Curvilinear flow in $(-q_1)$ direction	
Coordinate relations and limits	$x = a \cosh q_1 \cos q_2 \sin q_3$ $y = a \sinh q_1 \sin q_2$ $z = a \cosh q_1 \cos q_2 \cos q_3$ $0 \le q_1 \le q_1^f, \quad q_1^f = \sinh^{-1}\left(\frac{Y}{a}\right)$ $0 \le q_2 \le \pi/2$ $0 \le q_3 \le 2\pi$
Scale factors	$h_1^2 = h_2^2 = a^2(\cosh^2 q_1 - \cos^2 q_2)$ $h_3 = a \cosh q_1 \cos q_2$
Medium area	$A^0 = \pi a^2$
Cake volume	$V_c = \frac{2\pi a^3}{3}(\sinh q_1^f + \sinh^3 q_1^f)$
Shape factor	$h = 3/4$
Dimensionless pressure gradient	$J_0 = \frac{a}{P_c}\left(\sinh q_1^f + \sinh^3 q_1^f\right)\left(\frac{\partial P}{\partial y'}\right)_{y'=0}$
Cylindrical cake: Curvilinear flow in the $(-r)$ direction	
Coordinate relations and limits	$x = r \cos \theta, \quad R^0 \le r \le R^e$ $y = r \sin \theta, \quad 0 \le \theta \le 2\pi$ $z = z, \quad 0 \le z \le Z$
Scale factors	$h_r = h_z = 1, \quad h_\theta = r$
Medium area	$A^0 = 2\pi R^0 Z$
Cake volume	$V_c = \pi Z(R^{e2} - R^{02})$
Shape factor	$h = 1$
Dimensionless pressure gradient	$J_0 = \frac{1}{P_c}\left(\frac{R^{e2} - R^{02}}{2R^0}\right)\left(\frac{\partial P}{\partial r}\right)_{r=R^0}$
Elliptic-cylindrical cake: Curvilinear flow in the $(-q_1)$ direction	
Coordinate relations and limits	$x = a \cosh q_1 \cos q_2$ $y = a \sinh q_1 \sin q_2$ $z = z$

(*continued*)

Downloaded At: 12:42 25 January 2011

TABLE 3 (*continued*)

Elliptic-cylindrical cake: Curvilinear flow in the $(-q_1)$ direction	
	$0 \le q_1 \le q_1^f, \quad q_1^f = \sinh^{-1}\left(\frac{Y}{a}\right)$
	$0 \le q_2 \le \pi$
	$0 \le z \le b$
Scale factors	$h_1^2 = h_2^2 = a^2(\cosh^2 q_1 - \cos^2 q_2)$
	$h_z = 1$
Medium area	$A^0 = 2ab$
Cake volume	$V_c = \frac{\pi a^2 b}{4} \sinh 2q_1^f$
Shape factor	$h = 8/\pi^2$
Dimensionless pressure gradient	$J_0 = \frac{a \sinh 2q_1^f}{2P_c}\left(\frac{\partial P}{\partial y'}\right)_{y'=0}$

In Table 3 the medium area, A^0, the cake volume, V_c, and the shape factor, h, are obtained directly from measurable quantities. They are determined either by inspection of the geometry or by evaluating Eqs. (17), (21), and (24).

Equation (23) must be transformed into terms of measurable quantities before the dimensionless pressure gradient, J_0, can be determined. This is done by applying the chain rule. For the rectangular and cylindrical cake geometries, the local pressure profile can be determined by direct measurement of the pressure at known locations in the q_1 (z or r) direction.

Experimentally, q_1 positions can be difficult to determine for making local measurements in the oblate-spheroidal and elliptic-cylindrical cake geometries. One simple way is to locate the probes along the y-axis which is an axis of symmetry. The local pressure measured at points along the y-axis, indicated by y', are used to determine the pressure profile in terms of y'. The chain rule is used again to transform the pressure gradient in q_1 into the gradient in y'. This expression becomes

$$J_0 = \frac{V_c}{P_c}\left(\frac{dq_1}{dV_p}\right)^0\left(\frac{dy'}{dq_1}\right)^0\left(\frac{\partial P}{\partial y'}\right)_{y'=0} \tag{31}$$

which is evaluated at $q_1 = 0$ and $y' = 0$.

EXPERIMENTAL EVALUATION

The orthogonal curvilinear filter cake equation, Eq. (25), is applied here to a rectilinear flow cake to determine the constitutive parameter, λ, for cakes of Lucite particles formed from slurries of Lucite in water. The

Downloaded At: 12:42 25 January 2011

performance of an elliptic-cylindrical filter cake is predicted by using the above value of λ. Comparison with experimental measurements shows that the predicted results are within the experimental accuracy and imply that λ for incompressible cakes is independent of the cake geometry.

Experimental Apparatus

A diagram of the apparatus used to run the filter experiments is shown in Fig. 3. The slurry is agitated in the slurry supply tank and is kept well mixed by pumping the slurry at a moderate rate through a recycle line which returns the slurry to the top of the tank. Part of the slurry separates from the recycle line and enters the filter assembly where it forms the cake. The filtrate exiting the assembly flows through a control valve and a flowmeter, and flows into a filtrate weighing tank.

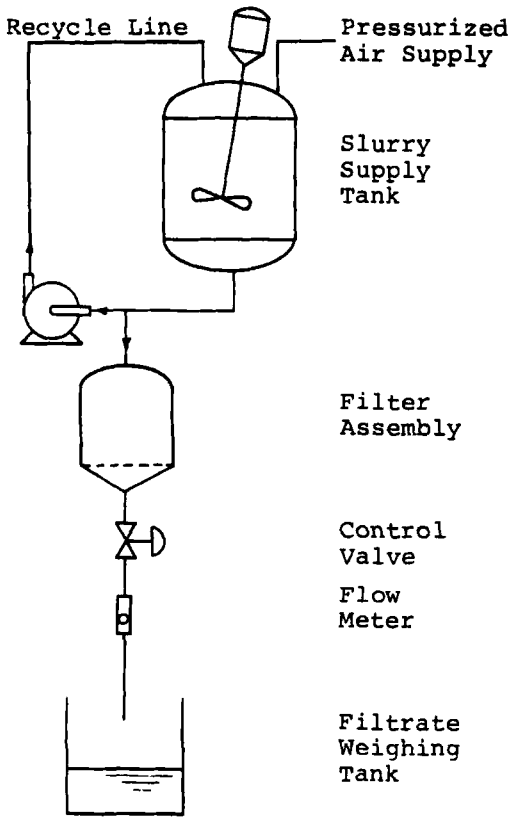

FIG. 3. Diagram of experimental apparatus.

Downloaded At: 12:42 25 January 2011

The experiments are run at constant flow rate. The constant flow rate is obtained by applying a constant air pressure to the free space in the slurry supply tank and by adjusting the control valve opening to obtain the desired flow rate. A computer monitors the flow rate via the flowmeter and makes adjustments to the valve opening as the filtration progresses.

An exploded sectional view of the filter assembly is in Fig. 4. The assembly body is constructed as a rectangular box made out of Plexiglas.

The filter medium and its support plate are locked into place at the

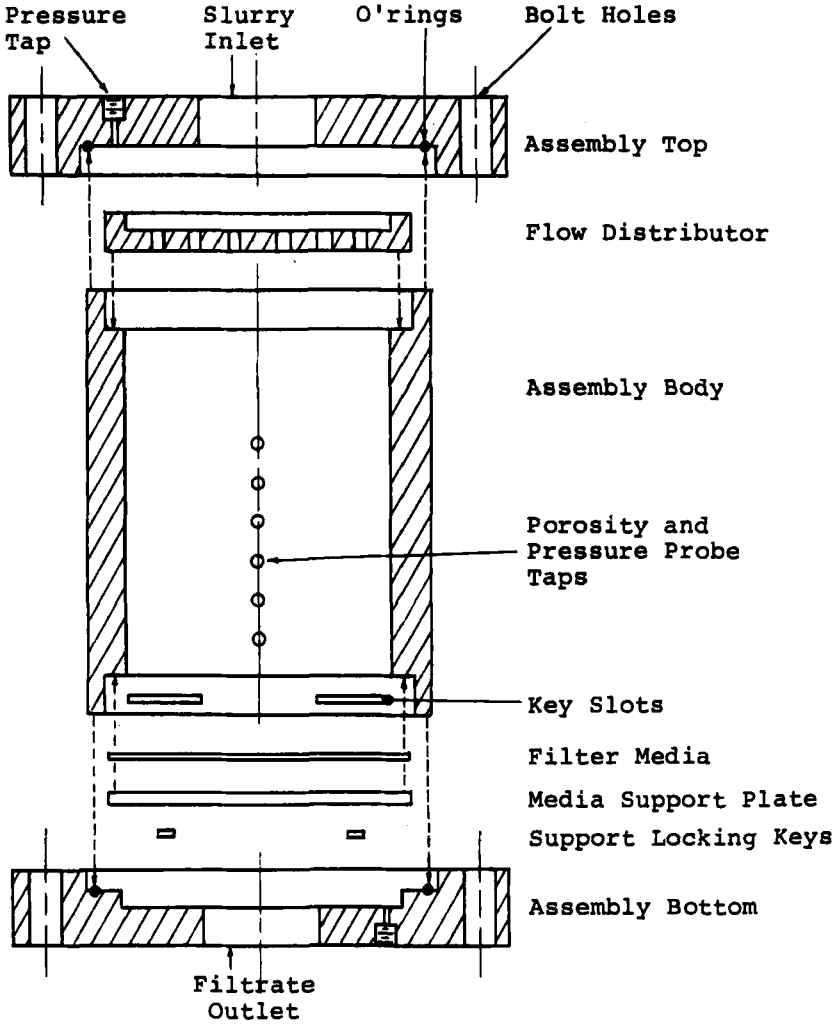

FIG. 4. Exploded sectional view of the filter assembly.

Downloaded At: 12:42 25 January 2011

bottom of the aseembly body by rotating two locking keys into key slots in the body walls. Rectilinear flow filter cakes are obtained when the entire filter medium surface is open to the approaching slurry in the filter assembly. Elliptic-cylindrical filter cakes are obtained when only the center portion of the medium is open to the approaching slurry, as shown in Fig. 5. In these latter cakes a thin sheet of plastic wrap is used to cover the portion of the medium surface that is closed to the flow.

Pressure taps and electroconductive porosity probes are aligned along the center line of the assembly walls. This center line corresponds to the y' positions needed for determining J_0 in the elliptic-cylindrical cake.

During each experiment the filter assembly is backlighted so that the cake forms a shadow in contrast to the slurry. A video camera is used to record the cake size and shape. A grid marked on the outer face of the assembly is used to determine the cake dimensions.

Experimental Results

The results of four experiments on rectilinear flow filter cakes are listed in Table 4. The results for these experiments indicate that the constitutive

Downloaded At: 12:42 25 January 2011

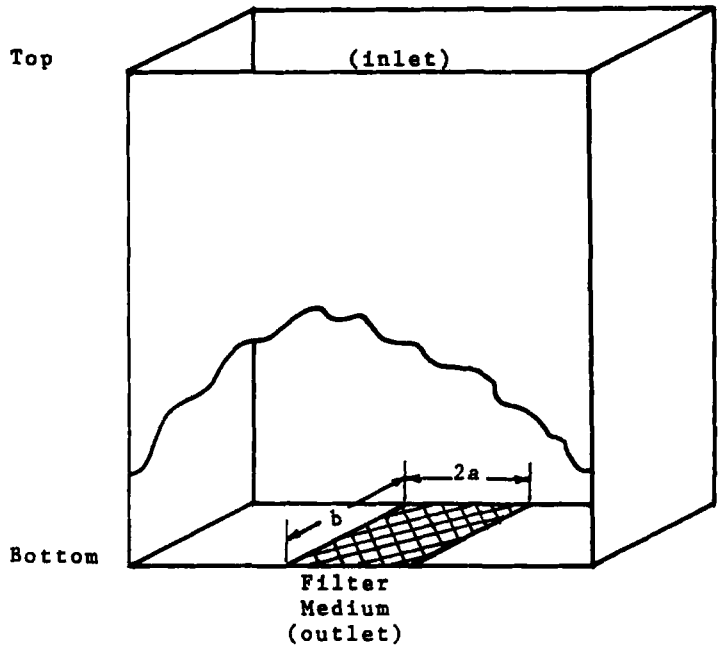

FIG. 5. Filter assembly for forming elliptic-cylindrical filter cakes. The cut-away view shows the inside of the assembly and the position of the filter medium.

TABLE 4
Experimental Results of Rectilinear Flow Filter Cakes

Experiment	$\dot{V}$ (m^3/s)	λ ($kPa \cdot s/m^2$)	$\pm\lambda$ uncertainty
1	1.33×10^{-3}	-5.3×10^4	0.53×10^4
2	1.33×10^{-3}	-5.5×10^4	0.61×10^4
3	0.83×10^{-3}	-5.9×10^4	0.65×10^4
4	0.33×10^{-3}	-5.8×10^4	0.93×10^4

parameter, λ, is reproducible within the experimental uncertainty and that it is independent of the flow rate.

The flow rate listed in Table 4 is the controlled flow rate set point. Initially the flow rate has fluctuations until the process is brought under control. The calculated values for the constitutive parameter, λ, presented in the table are the average values calculated using Eq. (25) after the flow rate fluctuations have subsided. The range of uncertainty of λ is determined from the uncertainties in the instrumental measurements.

For all four rectilinear flow experiments the porosity profiles are uniform and the pressure profiles are linear within experimental accuracy. This means that the Lucite cakes are incompressible and J_0 is unity, which simplifies the calculations. The complete experimental data for each of the experiments are given in the Appendix.

The average value of λ in the rectilinear flow experiments is -5.6×10^4 $kPa \cdot s/m^2$. Taking the experimental uncertainty into account gives a range of -4.8×10^4 to -6.7×10^4 $kPa \cdot s/m^2$ for λ. For this range of λ the product $P_c J_0$ is plotted in Fig. 6 as a function of the elliptic-cylindrical cake height, Y. This range of values of $P_c J_0$ is compared to the experimentally determined $P_c J_0$ where P_c is directly measured and J_0 is determined from the expression in Table 3 for the elliptic-cylindrical cake.

The $P_c J_0$ data points for values for Y greater than 0.025 m in Fig. 6 fall within the experimental uncertainty range of the estimated value for the constitutive parameter, λ. As expected for an incompressible cake, this result shows experimentally that λ is independent of the cake geometry. This also demonstrates the consistency of the orthogonal curvilinear filter cake equation between the cake geometries. The points for values of Y less than or equal to 0.025 m in Fig. 6 fall near but not within the uncertainty range in λ. The deviation of these latter points is most likely due to the initial fluctuations in the flow rate and the inaccuracy in determining the pressure gradient in the small filter cake.

The experimental apparatus used in this investigation does not submerge the filter assembly into a larger vessel in which the slurry is agitated as is done in the literature (*2*, *3*, *7*, *11*, *12*, *14*, *15*). This design allows ready access to the assembly walls for placement of pressure and porosity probes.

Downloaded At: 12:42 25 January 2011

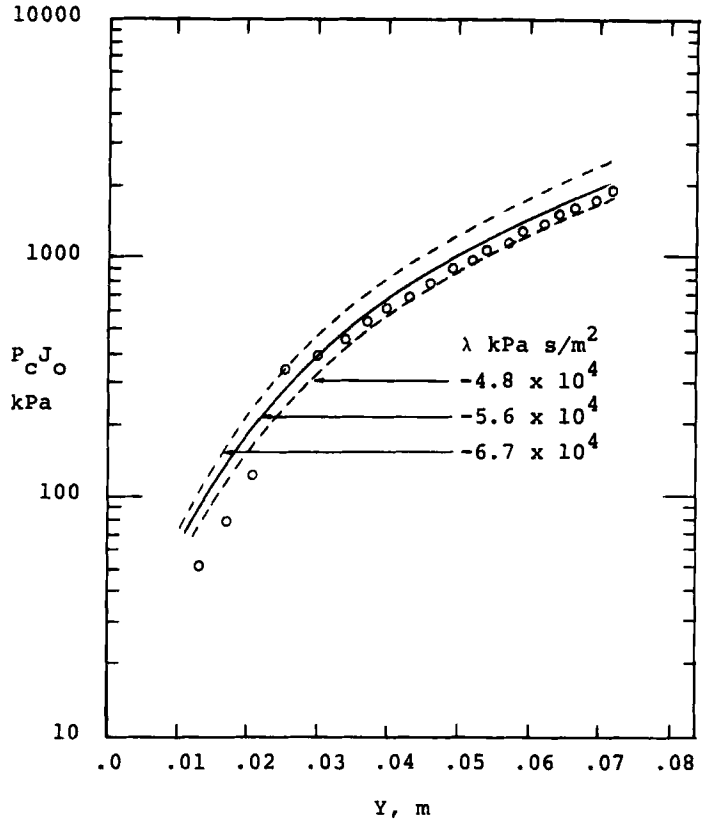

FIG. 6. Comparison of predicted and experimental P_cJ_0 vs Y data for the elliptic-cylindrical filter cake. The solid curve represents the predicted values calculated from the average λ value of -5.6×10^4 kPa·s/m^2. The broken curves indicate the extent of the uncertainty in λ, from -4.8×10^4 to -6.7×10^4 kPa·s/m^2. The individual points are from the experimental data.

However, it does have a drawback in that some of the particles settle out of the slurry, which does not occur when the assembly is submerged in an agitated vessel. This effect is shown in Fig. 7 where the outer edges of the cake deviate from the idealized elliptic-cylindrical shape. From the experimental results it appears that the settling does not significantly affect the measurements.

CONCLUSIONS

The orthogonal curvilinear filter cake equation that is derived here can be applied to any orthogonal curvilinear cake geometry. This is demonstrated by applying the equation to rectangular, cylindrical, oblate-cylin-

Downloaded At: 12:42 25 January 2011

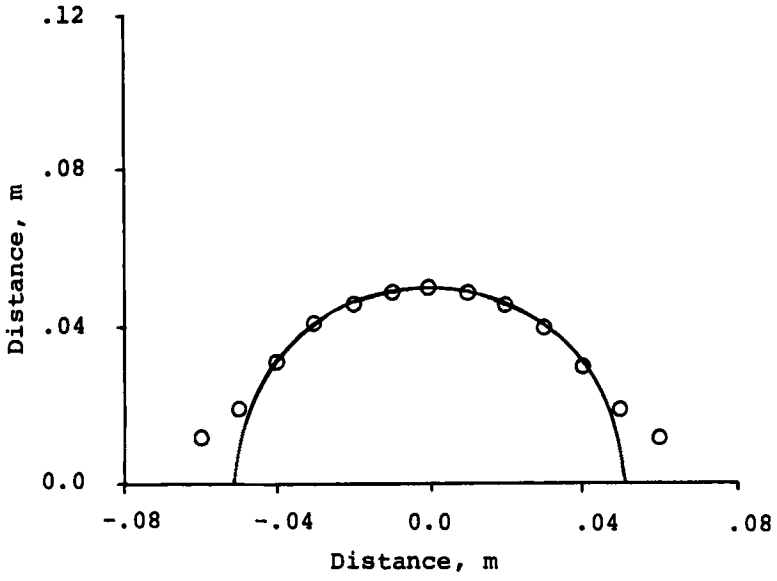

FIG. 7. Comparison of the surface of the experimental elliptic-cylindrical filter cake (discrete points) at $Y = 0.05$ m and $a = 0.01$ m to the ideal elliptic-cylindrical surface (continuous curve).

Downloaded At: 12:42 25 January 2011

drical, and elliptic-cylindrical filter cakes. The terms in the equation, such as the shape factor, h, and the dimensionless pressure gradient, J_0, are related directly to measurable quantities.

The orthogonal curvilinear filter cake equation is tested on rectangular and elliptic-cylindrical filter cakes. Local pressure measurements are used to determine the dimensionless pressure gradient, and local porosity measurements are used to verify the uniformity of the local porosity. The experimental results show that within the experimental uncertainty λ is independent of the cake geometry for incompressible cakes.

Possible future research in this area include extending this work to cakes of nonuniform porosity and to other geometric conditions. The nonuniform porosity profile will have an effect on the constitutive parameter, λ, and on the dimensionless pressure gradient, J_0, for different cake geometries. Other geometric conditions that could be investigated include other coordinate directions (such as the θ direction in cylindrical coordinates), other curvilinear coordinate geometries, and the effects of interacting coordinate geometries (such as when multiple oblate-spheroidal cakes grow on a surface and come into contact, which occurs on a Buchner funnel).

APPENDIX

Experimental data on Lucite filter cakes are provided in this Appendix. The first four experiments are in rectangular geometry and the fifth experiment is in elliptic-cylindrical geometry. All of the experiments are run at constant rate and with a Whatman 4 filter medium. The solid Lucite particle phase has an intrinsic density of 1.175 g/cm^3. The fluid phase is water with an approximate density of 0.997 g/cm^3, depending on the filtrate temperature.

Experimental conditions, such as the slurry porosity, cake average porosity, and the temperature, are listed in Table 5. Also listed in this table for the rectangular geometry cakes are the mean values of the constitutive parameter, λ, and the estimated relative uncertainties. The mean values are determined from the experimental data after initial fluctuations in the flow rate have subsided. The relative uncertainties are determined from the estimated uncertainties in the experimental measurements.

The time and positionally dependent data are plotted in Figs. 8 through 12. The macroscale variables (V, $\dot{V}$, and P_c) are plotted as functions of cake height. The local measurements are plotted as functions of position or dimensionless position and cake height.

In the plots of the macroscale variables the magnitudes of the macro variables are scaled by multiplying by the powers of 10 shown on the ordinate axis. The true values of the variables can be obtained by dividing the values on the plot by 10 to the given exponential power.

The local pressure is plotted as functions of local position and cake height. In these plots the listed cake heights represent the moment in time for which the profiles are plotted. The smallest cake height in the list corresponds to the left-most pressure profile. Within the accuracy of the pressure probes (±2 kPa), the pressure profiles in Figs. 8 through 11 are linear.

Within the accuracy of the porosity probes (±0.05), the local porosity is uniform and constant in each of the experiments. This is shown in the local porosity plots in Figs. 8 through 12. The local porosity in these figures is plotted as a function of dimensionless position, z/L or y'/Y. Due to the uniformity of the porosity, no distinction is made between the moments in time for the porosity data.

NOTATION

A area of a constant q_1 surface, Eq. (21)
a radius or half-width of filter media, Fig. 2
b width of the elliptic-cylindrical cake in Fig. 2
G cake-filtrate volume ratio, Eq. (26)
$\mathbf{g}$ gravity acceleration

Downloaded At: 12:42 25 January 2011

Downloaded At: 12:42 25 January 2011

TABLE 5
Experiment Conditions. Experiments 1 through 4 Are Rectangular Geometry Cakes, and Experiment 5 is an Elliptic-Cylindrical Geometry Cake

Experiment	1	2	3	4	5
Slurry porosity, ϵ_f	0.938	0.976	0.939	0.936	0.974
Cake average porosity, ϵ_f^*	0.391	0.372	0.393	0.402	0.377
Volume ratio, G	0.118	0.035	0.111	0.117	0.041
Medium area, A^0 (m^2)	4.09×10^{-3}	3.87×10^{-3}	4.09×10^{-3}	4.09×10^{-3}	5.08×10^{-4}
Temperature, T (°C)	21.3	24.6	21.0	20.5	24.6
Flow rate set point, $\dot{V}$ (m^3/s)	1.33×10^{-5}	1.33×10^{-5}	0.83×10^{-5}	0.33×10^{-5}	0.83×10^{-5}
Constitutive parameter, λ ($kPa \cdot s/m^2$)	-5.3×10^4	-5.5×10^4	-5.9×10^4	-5.8×10^4	—
Parameter relative uncertainty, $\Delta\lambda/\lambda$	0.10	0.11	0.11	0.16	—

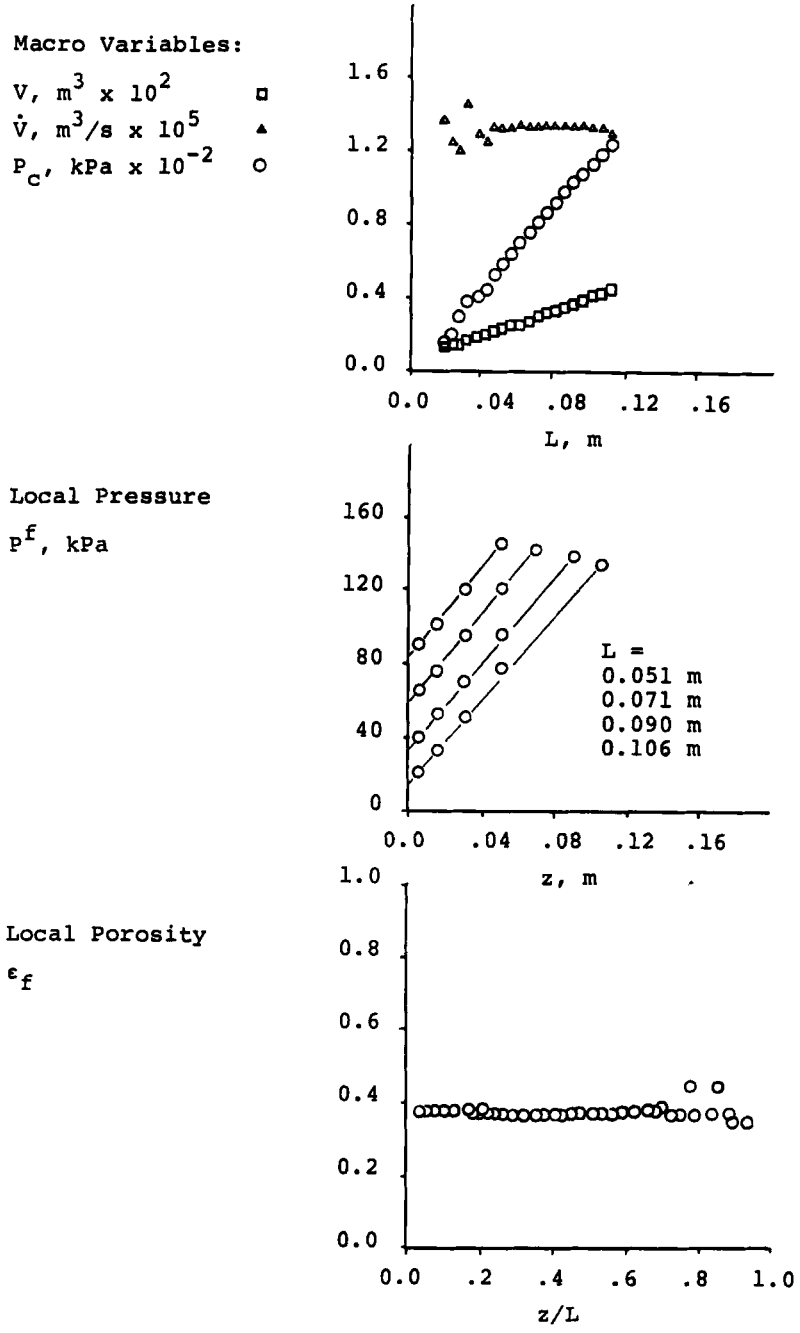

FIG. 8. Plots of data from Experiment 1: constant rate 1.33 × 10^{-5} m^3/s rectilinear flow in a rectangular cake geometry.

Downloaded At: 12:42 25 January 2011

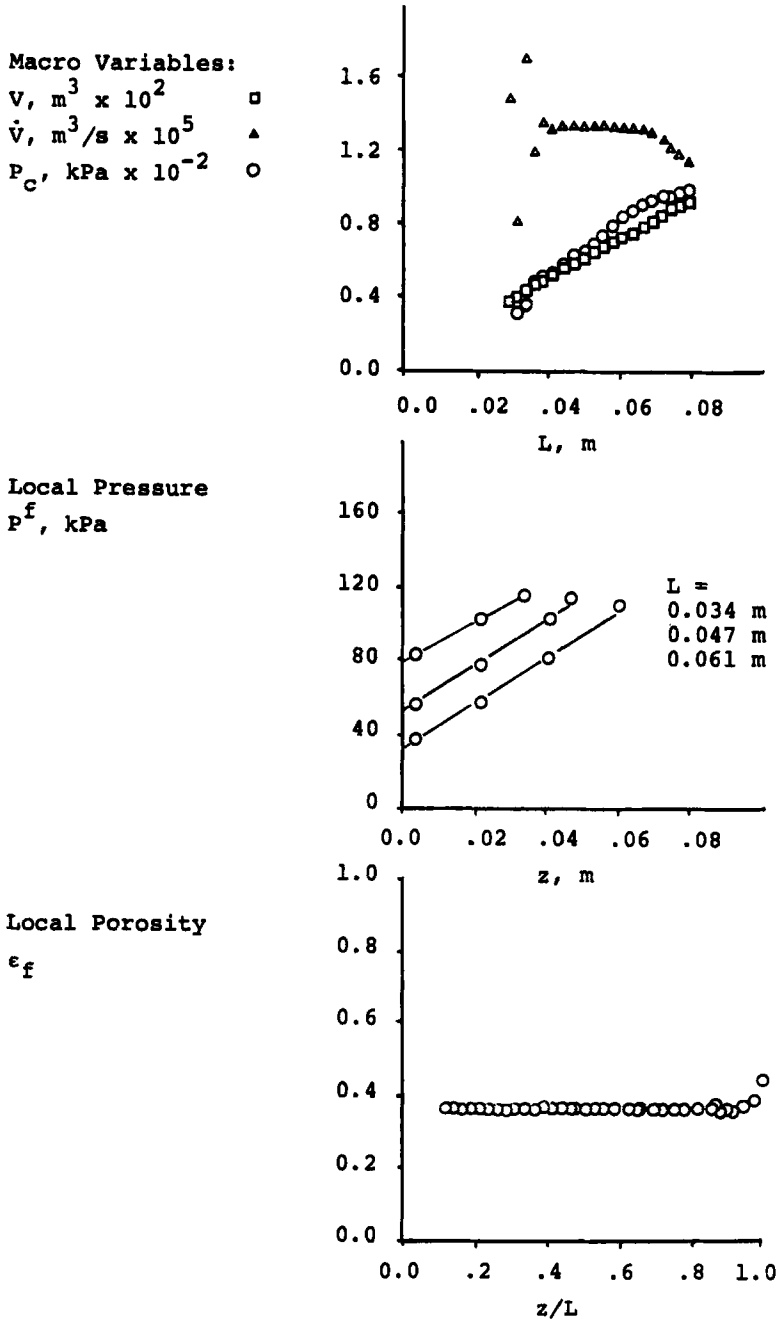

FIG. 9. Plots of data from Experiment 2: constant rate 1.33×10^{-5} m³/s rectilinear flow in a rectangular cake geometry.

Downloaded At: 12:42 25 January 2011

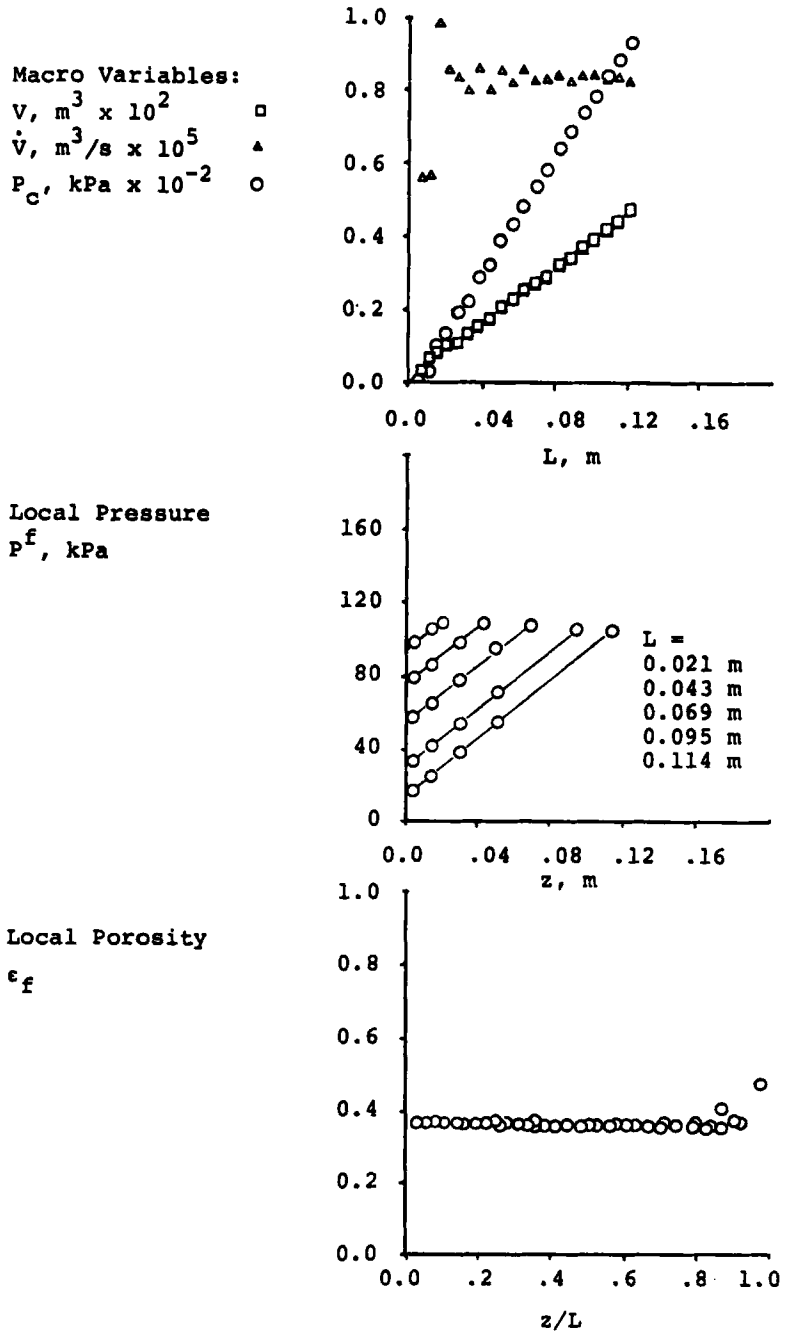

FIG. 10. Plots of data from Experiment 3: constant rate 0.83 × 10^{-5} m^3/s rectilinear flow in a rectangular cake geometry.

Downloaded At: 12:42 25 January 2011

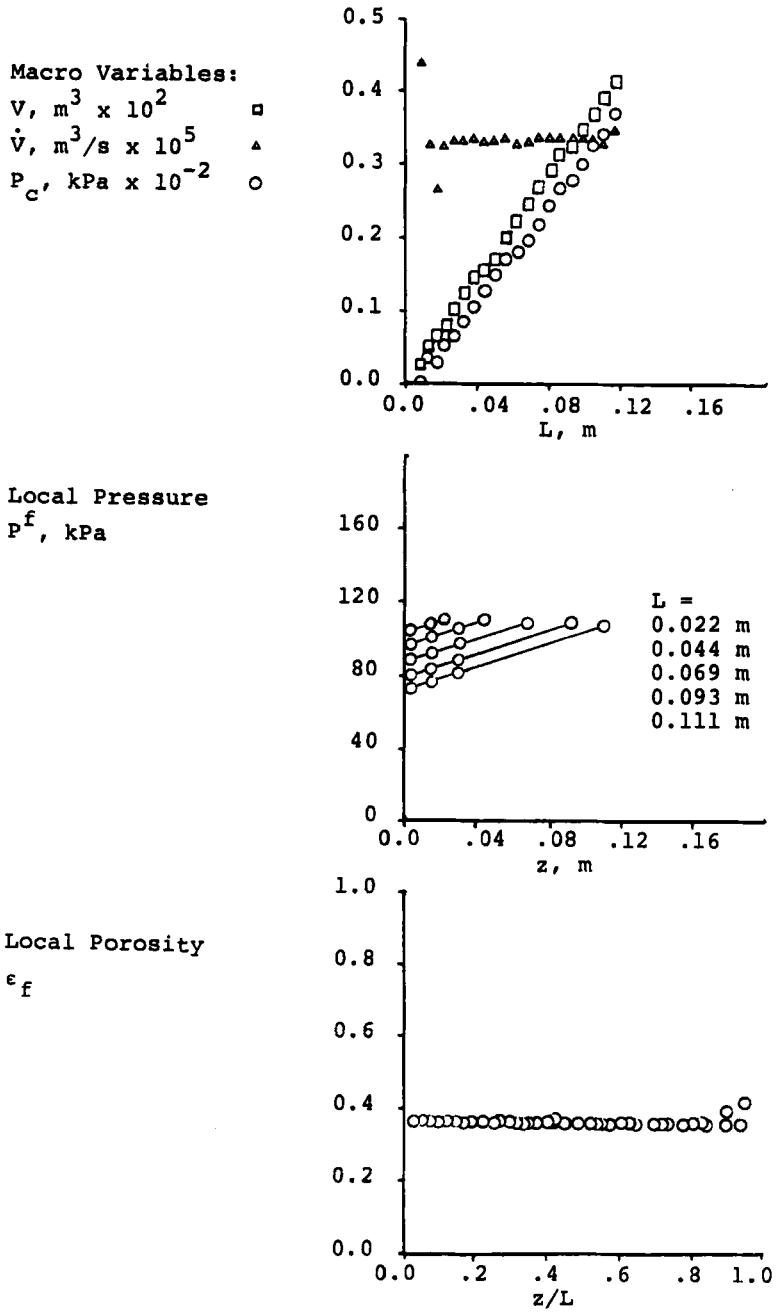

FIG. 11. Plots of data from Experiment 4: constant rate 0.33 × 10^{-5} m^3/s rectilinear flow in a rectangular cake geometry.

Downloaded At: 12:42 25 January 2011

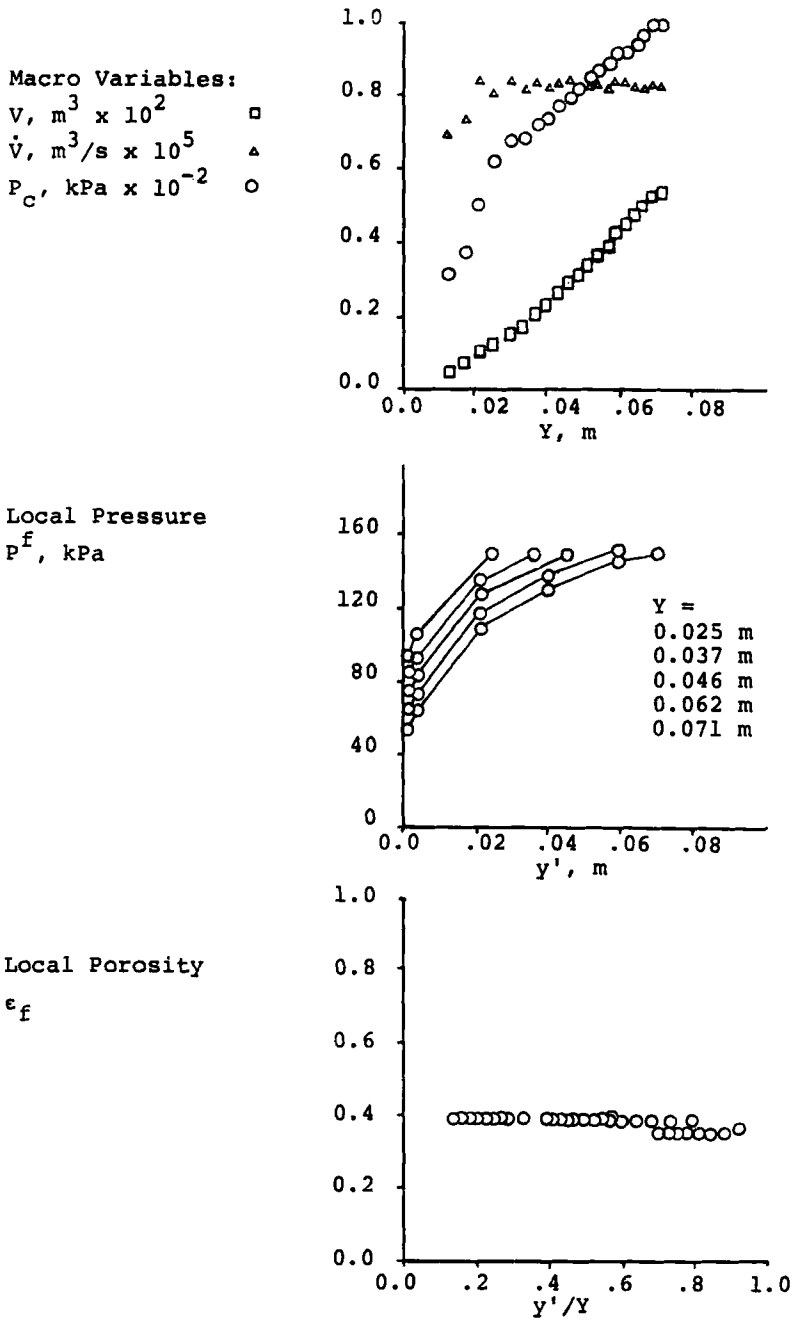

FIG. 12. Plots of data from Experiment 5: constant rate 0.83 × 10^{-5} m^3/s curvilinear flow in an elliptic-cylindrical cake geometry.

Downloaded At: 12:42 25 January 2011

h shape factor, Eq. (24)
h_i curvilinear coordinate scale factor
J_0 dimensionless pressure gradient, Eq. (23)
L rectangular geometry cake height, Fig. 2
p^f fluid phase pressure
P_c pressure drop across the filter cake
q_k kth coordinate of the (q_1,q_2,q_3) coordinate system
q_k^e upper or external boundary position of cake in q_k direction
q_k^0 lower boundary position of cake in q_k direction
$\hat{\mathbf{T}}^\alpha$ interphase momentum transfer vector function
$\mathbf{t}^\alpha$ α-phase stress tensor
V filtrate volume
$\dot{V}$ filtrate volumetric flow rate
V_c cake volume
V_p partial cake volume, Eq. (17)
v_k^α kth component of the intrinsic α-phase average velocity
$\mathbf{v}^\alpha$ intrinsic α-phase average velocity
X dimension of filter cakes in x-direction, Fig. 2
Y dimension of filter cakes in y-direction, Fig. 2
y' positions along the y-axis
Z dimension of filter cakes in z-direction, Fig. 2

Greek Letters

ϵ_α α-phase porosity
$\boldsymbol{\lambda}$ material coefficient tensor for the interphase drag force $\hat{\boldsymbol{\tau}}^\alpha$
ξ dimensionless position, Eq. (16)
ρ^α α-phase intrinsic density
$\boldsymbol{\tau}^\alpha$ α-phase dissipative stress tensor
$\hat{\boldsymbol{\tau}}^\alpha$ interphase drag force

Superscripts/Subscripts

f denotes fluid phase
s denotes solid phase
0 quantity is evaluated at the medium, at q_1^0
α denotes either the fluid or solid phase

Acknowledgment

The financial assistance from the Department of Chemical Engineering at The University of Akron is gratefully acknowledged.

Downloaded At: 12:42 25 January 2011

REFERENCES

1. Bachmat, Y., and J. Bear, "Mathematical Formulation of Transport Phenomena in Porous Media," in *Proceedings of the Symposium on Fundamentals of Transport Phenomena in Porous Media,* Vol. 1, Guelph, Ontario, Canada, 1972, p. 174.
2. Brenner, H., "Three-Dimensional Filtration on a Circular Leaf," *AIChE J., 7*(4), 666 (1961).
3. Bybyk, S., "The Effect of Filter Cake Geometry on the Multiphase Filtration Theory," Master's Thesis, The University of Akron, Ohio, 1985.
4. Chase, G. G., "Continuum Analysis of Constant Rate Cake Filtration," PhD Dissertation, The University of Akron, Ohio, 1989.
5. Carbonell, R. G., and S. Whitaker, "Heat and Mass Transfer in Porous Media," in *Fundamentals of Transport Phenomena in Porous Media* (J. Bear and M. Y. Corapciogly, eds.), Nijhoff, The Hague, The Netherlands, 1984, p. 121.
6. Desai, F. N., "Balance Equations and Constitutive Equations for Porous Media Flows with Large Porosity Gradients," PhD Dissertation, The University of Akron, Ohio, 1989.
7. Gregor, W., and B. Scarlett, "3 Dimensional Filtration and its Importance in Equipment Design," *Filtr. Sep., 11*(2), 151 (1974).
8. Hassanizadeh, M., and W. G. Gray, "General Conservation Equations for Multi-phase Systems: 1. Averaging Procedure," *Adv. Water Resour., 2*(3), 131 (1979).
9. Hassanizadeh, M., and W. G. Gray, "General Conservation Equations for Multi-phase Systems: 2. Mass, Momentum, Energy and Entropy Equations," *Ibid., 2*(4), 191 (1979).
10. Hassanizadeh, M., and W. G. Gray, "General Conservation Equations for Multi-phase Systems: 3. Constitutive Theory for Porous Media Flow," *Ibid., 3*(1), 25 (1980).
11. Leonard, J. I., and H. Brenner, "Experimental Studies of Three-Dimensional Filtration on a Circular Leaf," *AIChE J., 11*(6), 965 (1965).
12. Murase, T., K. Kobayashi, E. Iritani, K. Ito, and M. Shirato, "Constant-Pressure Filtration on Cylindrical Surfaces of Power-Law Non-Newtonian Fluids," *J. Chem. Eng. Jpn., 18*(3), 230 (1985).
13. Pearson, C. E., *Handbook of Applied Mathematics,* Van Nostrand Reinhold, New York, 1974.
14. Shirato, M., and K. Kobayashi, *Fundamental Concepts for non Uni-Dimensional Filtration,* Presented at the 64th National AIChE Meeting, New Orleans, Louisiana, 1969.
15. Shirato, M., T. Murase, and K. Kobayashi, "The Method of Calculation for Non Uni-Dimensional Filtration," *Filtr. Sep., 5*(3), 219 (May/June 1968).
16. Slattery, J. C., *Momentum, Energy and Mass Transfer in Continua,* McGraw-Hill, New York, 1972.
17. Tiller, F. M., and C. S. Yeh, "The Role of Porosity in Filtration, Part X: Deposition of Compressible Cakes on External Radial Surfaces," *AIChE J., 31*(8), 1241 (1985).
18. Willis, M. S., R. M. Collins, and W. G. Bridges, "Complete Analysis of Non-Parabolic Filtration Behavior," *Chem. Eng. Res. Des., 61*(2), 96, (1983).
19. Willis, M. S., M. Shen, and K. J. Gray, "Investigating the Fundamental Assumptions Relating Compression-Permeability Data with Filtration," *Can. J. Chem. Eng., 52*(3), 331 (1974).
20. Willis, M. S., and I. Tosun, "A Rigorous Cake Filtration Theory," *Chem. Eng. Sci., 35*(12), 2427 (1980).
21. Yoshioka, N., K. Ueda, and K. Miyoshi, "Liquid Pressure Distribution for Filtration through Curved Leaves," *J. Chem. Eng. Jpn., 5*(3), 291 (1972).

Received by editor March 20, 1990

Downloaded At: 12:42 25 January 2011